

Rapid imaging of nanotubes on insulating substrates

T. Brintlinger, Yung-Fu Chen, T. Dürkop, Enrique Cobas, and M. S. Fuhrer^{a)}
Department of Physics, University of Maryland, College Park, Maryland 20742

John D. Barry and John Melngailis
Institute for Research in Electronics and Applied Physics, College Park, Maryland 20742

(Received 31 May 2002; accepted for publication 30 July 2002)

We demonstrate the use of field-emission scanning electron microscopy for rapid imaging of small-diameter carbon nanotubes on insulating SiO₂ substrates. The image contrast stems from local potential differences between the nanotube and substrate and is insensitive to surface roughness and defects. This technique may also be used as a probe of the electrical connectivity of small structures without external leads. © 2002 American Institute of Physics. [DOI: 10.1063/1.1509113]

Since the discovery of single-walled and multiwalled carbon nanotubes (NTs),^{1,2} their promise as a basis for molecular electronics has been extensively investigated. Already, NT devices have yielded field-effect transistors,^{3,4} single-electron tunneling transistors,^{5,6} rectifiers,⁷⁻⁹ and simple logic devices.^{10,11} However, to proceed to a useful technology, methods are needed to place NTs with precision on insulating substrates; such methods are the subject of much current research. The scanning probe microscope (SPM) is now the primary tool for locating, identifying, and characterizing carbon NTs. While very effective, using an SPM to assay the production of NTs or their placement on a substrate is time consuming, and is often a bottleneck in NT device research. In this letter, we show how a field-emission scanning electron microscope (FESEM) can rapidly image the locations and electrical connectivity of NTs with insensitivity to surface contamination. In this mode, the FESEM acquires scans 2–3 orders of magnitude quicker than an SPM. This technique relies on the differential charging of the conducting NTs and insulating substrate, and is, therefore, much more robust to surface defects than the SPM. We expect this technique to be generally useful in imaging nanoscale conducting objects on insulators.

The nanotubes in this study were prepared as part of a larger ongoing research effort to fabricate and study the electronic properties of single NT devices. However, the technique outlined here should be of general utility to researchers studying the synthesis, self-assembly, and alignment of any conducting nanowires on insulating substrates. Using chemical vapor deposition, carbon NTs were grown directly on oxidized silicon substrates.¹²⁻¹⁴ The process used here produces 1–5 nm diameter, ~1–100 μm long NTs distributed randomly on the surface. In order to locate individual NTs for electrical contacting, a conventional electron-beam lithography lift-off process is used to pattern Cr/Au alignment markers on the substrate. Typically, NTs are located relative to the alignment marks using an atomic force microscope (AFM); this is the most time-consuming step in fabricating single-NT devices, prompting us to explore other imaging techniques.

Figure 1 compares images of the same set of NTs and alignment markers taken with an FESEM [Fig. 1(a)] and intermittent-contact mode AFM [Fig. 1(b)]. Two isolated NTs may be seen in each image as well as the Cr/Au alignment markers. In many similar scans, no NTs were detected by AFM that were previously undetected by the FESEM. The NTs and alignment markers lie on 500 nm of SiO₂; no conductive coating was used to enhance the image. In the FESEM scan, the NTs appear in the same location as in the AFM scan, but their apparent diameters (~50 nm) are much larger than the AFM height profile indicates (1–2 nm), in fact, larger than the spot size of the electron beam. Also in Figs. 1(a) and 1(b), the general surface contamination appearing in the AFM image does not appear in the corresponding FESEM image. This behavior exists in all such images: The FESEM detects contrast for conducting areas on the substrate (corresponding to the NT location), but not for other nonconducting areas, even those with considerable surface roughness. These facts suggest that the contrast mecha-

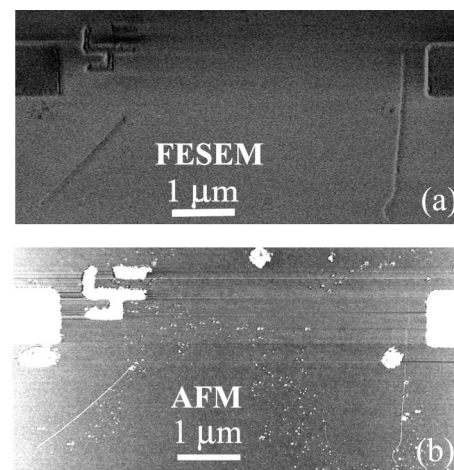


FIG. 1. Comparison of AFM and FESEM images of the same NTs. (a) Zeiss DSM982 FESEM operating at 1 kV with 20 pA beam current using in-lens secondary-electron detector. The entire $12 \times 12 \mu\text{m}^2$ image was acquired in ~10 s; a portion is shown. (b) Topograph from JEOL JSPM-4210 AFM operating in intermittent-contact mode. The entire $10 \times 10 \mu\text{m}^2$ image was acquired in ~700 s; a portion is shown. Both images show two isolated NTs (lengths 2 and 3 μm, and diameters 2.2 and 0.9 nm, respectively, for the left- and right-hand side NTs), as well as $1 \mu\text{m}^2$ gold pads and gold alignment markers.

^{a)}Author to whom correspondence should be addressed; electronic mail: mfuhrer@physics.umd.edu

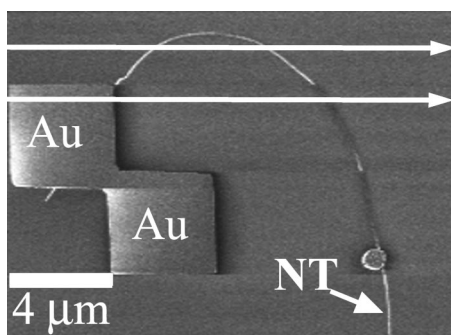


FIG. 2. FESEM image of NT connected to a gold pad. The beam is moving from the left- to right-hand side at a linear speed of $\sim 500 \mu\text{m/s}$, and slowly from top to bottom. The horizontal arrows draw attention to particular scan lines: During the line scan corresponding to the upper arrow, the beam crosses the NT, but not the gold pad. The NT appears brighter than the surrounding oxide substrate. During the line scan corresponding to the lower arrow the beam crosses the gold pad before crossing the NT, and the NT appears dark in comparison with the surrounding oxide.

nism does not depend on direct backscattering of the electron beam by the carbon lattice of the NT.

Figure 2 shows an FESEM image of a NT connected to an electrically isolated gold pad. The beam is scanned from the left- to right-hand side at linear speed of $\sim 500 \mu\text{m/s}$, and sequential line scans are taken from top to bottom. We draw attention to two particular line scans, represented by the horizontal arrows in Fig. 2. In the upper line scan, a NT is scanned without simultaneously scanning a large conducting pad; the NT appears brighter than the surrounding substrate. In the lower line scan in Fig. 2, a large pad is scanned previous to a NT connected to that pad. The NT now shows the opposite contrast, appearing darker than the surrounding substrate.

We interpret the contrast changes observed in Figs. 1 and 2 as follows. It is known that thick SiO_2 is charged negatively when scanned by the electron beam.^{15,16} Differences in surface electrostatic potential affect the number of secondary electrons leaving the SiO_2 : A positive surface potential will increase the number of secondaries, in effect, pulling them out of the oxide, while a negative surface potential will decrease the number of secondaries.¹⁷ Excepting the gold features, we interpret the bright (dark) contrast in Figs. 1 and 2 as due to increased (decreased) secondary-electron emission from the SiO_2 arising from positive (negative) surface potentials relative to the SiO_2 bulk; i.e., the image is obtained by voltage contrast.

We use this voltage contrast model to explain the observed features in Fig. 2. We assume that the interaction of the electron beam with the NT is negligible, and the nanotube acquires electrical charge only through conduction through the SiO_2 substrate. The large capacitance conducting NT charges negatively much more slowly than the surrounding surface and, therefore, is at a positive potential relative to the oxide bulk (i.e., charge reaching the NT will be distributed over its length). Thus, the NT first appears bright in the upper line scan of Fig. 2. The NTs have an apparent width of $\sim 50\text{--}100 \text{ nm}$ in the FESEM images, much greater than the $1\text{--}5 \text{ nm}$ diameters measured by AFM. This further indicates that the detected secondary electrons have been affected by the electric field of the nanotube: The field lines produce a much larger effective diameter. In the lower line scan of Fig. 2, the beam crosses the gold pad before crossing the NT, and the NT appears dark in comparison with the surrounding oxide.

2, the beam crosses the gold pad before crossing the NT. Here, the gold pad acquires a significant negative charge from the beam, as evidenced by the dark contrast in the oxide near the beam, at the trailing edge of the gold pad. Because the nanotube is electrically connected to the pad, it is at a relatively negative potential when scanned by the beam and, thus, appears dark. A similar effect causes the portion of the NT at the top of the image which is nearly parallel to the scan direction to show reduced contrast; the beam is over the NT for a longer duration, and some charging of the nanotube occurs, reducing the contrast.

The aforementioned observations clearly show that differences in surface electrostatic potential are responsible for the contrast between the NT and substrate observed in the FESEM. Voltage contrast is well known in electron microscopy,¹⁷ but is typically accomplished using externally biased electrical connections to features on the sample. Here, voltage contrast is produced without external electrical connections.

Because there are no external leads, the voltage contrast arises dynamically, leading to important consequences. Decreasing scan speed, increasing magnification, or increasing beam current is found to *reduce* the image contrast. These changes all enhance the effect of charging, causing the NT to come closer to potential equilibrium with the substrate, thus decreasing contrast. We also find that the image contrast is highest at accelerating voltages of $1\text{--}2 \text{ kV}$; dropping significantly for voltages $>3 \text{ kV}$. At these accelerating voltages, negative charging of the substrate is typically minimized: The ratio of primary to secondary electrons approaches unity for thick oxides.¹⁵ Additionally, at higher accelerating voltages, the beam penetrates deeper into the oxide, producing less secondary electrons near the surface which would be sensitive to surface potential differences.

Although our sample contains both metallic and semi-conducting NTs, we have not seen evidence for two different types of NTs in our FESEM images. The dynamic voltage contrast requires that the charge disperses along the NT more rapidly than the charge arrives at the nanotube. We estimate that the characteristic time for the NT to reach potential equilibrium with the oxide is greater than $10 \mu\text{s}$, the longest dwell time of the beam near the NT for which contrast is still observed. Experimentally, we observe a resistance on order $10^5 \Omega/\mu\text{m}$ at zero gate voltage for semiconducting NTs, while the off-state resistance is typically $<10^{10} \Omega/\mu\text{m}$. The capacitance per length of the NTs is approximately $10^{-17} \text{ F}/\mu\text{m}$, from which we obtain a time constant of $<10^{-9} \text{ s}$ for a 100 nm section of NT (approximating the area over which secondary electrons are affected by the NT potential). This is significantly less than the equilibration time, thus, we expect even the most resistive semiconducting NTs to appear conductive. A more rigorous estimate of the maximum resistance object which could be observed by our technique would require more detailed knowledge of the proper length scale to consider herein; in principle, this could be obtained experimentally by determining the shortest possible segments of NT which can be imaged.

The imaged diameter of NTs in our samples is $50\text{--}100 \text{ nm}$, much greater than their physical diameter of $1\text{--}5 \text{ nm}$. Because the voltage contrast mechanism is sensitive to the

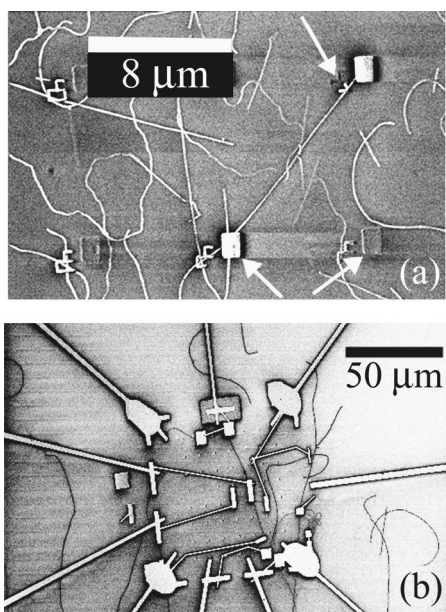


FIG. 3. Electrical connectivity imaging with the FESEM. (a) Image of a substrate with NTs and a regular array of $1 \mu\text{m}^2$ square alignment markers and smaller symbols. The square alignment markers which are contacted by NTs show significantly greater contrast with the oxide substrate (compare markers indicated by two bottom arrows). Alignment markers which are not connected to NTs are nearly undetected. The small symbols are made up of 150 nm wide gold lines. One symbol is connected to a nanotube (arrow on upper right-hand side) and shows evidence of an electrical break: Only a portion of the symbol shows contrast with the oxide. Scale bar = $8 \mu\text{m}$. (b) Low magnification FESEM image of substrate with large gold bonding pads and interconnects. A long-range electrical short caused by a single NT is visible on the left-hand side. Scale bar = $50 \mu\text{m}$. Aside from a difference in background due to autocontrasting, a comparison of (a) and (b) also shows evidence for the contrast inversion displayed in Fig. 2: The NTs connected to large pads in (b) appear very dark after they have been charged by the beam, while the NTs in (a) are lighter as they discharge to NTs and pads outside the scan area.

long-range electric field around the NT, we expect that diameter information will be difficult to obtain from this technique.

However, the imaging technique described here does have advantages. As with conventional voltage contrast,¹⁷ the technique described here may be used as a continuity/connectivity probe, but one that does not require external leads for voltage biasing. Figure 3(a) shows a regular array of gold alignment markers, some of which are connected to NTs. The gold islands which are contacted by NTs are brighter than uncontacted ones (compare markers indicated by lower two arrows). Following the rationale outlined in regard to Fig. 2: Because gold islands connected by NTs have a larger total capacitance than uncontacted islands, the same amount of charge results in more potential difference relative to the oxide, which produces more contrast. Similar to Fig. 2, some changes in NT contrast are observed when the beam scans across a connected gold island. Also in Fig. 3(a): It is possible to see a ($<50 \text{ nm}$) break in the gold

alignment mark (top right-hand side arrow). The contacted portion is brighter than the uncontacted portion, just as in externally biased voltage contrast. In Fig. 3(b), a low magnification image shows a rather long NT shorting two gold leads between NTs within the alignment mark grid and larger bonding pads (outside the field of view). The large wires and pads charge the connected NTs, suppressing secondary-electron emission and causing them to appear dark. Figure 3(a) displays the usefulness of such a connectivity probe for detecting long-range electrical shorts: Long conducting NTs connected to metal pads may be imaged at very low magnification. Such large scan areas would be prohibitively time consuming with conventional AFM scanning. The enhanced contrast for small conducting objects when they are connected by NTs [e.g., Fig. 3(a)] also hints that NTs might provide an alternate conducting coating when spun on a non-conducting sample from solution; in some circumstances, this may be less invasive than the evaporation of conducting films such as gold or carbon.

This research was supported by ARDA and the Office of Naval Research through Grant No. N000140110995, and the National Science Foundation through Grant No. DMR-0102950.

- ¹S. Iijima, *Nature (London)* **354**, 56 (1991).
- ²M. S. Dresselhaus, G. Dresselhaus, and P. C. Eklund, *Science of Fullerenes and Carbon Nanotubes* (Academic, San Diego, 1996).
- ³S. J. Tans, R. M. Verschueren, and C. Dekker, *Nature (London)* **393**, 49 (1998).
- ⁴R. Martel, T. Schmidt, H. R. Shea, T. Hertel, and P. Avouris, *Appl. Phys. Lett.* **73**, 2447 (1998).
- ⁵S. J. Tans, M. H. Devoret, H. Dai, A. Thess, R. E. Smalley, L. J. Georluga, and C. Dekker, *Nature (London)* **386**, 474 (1997).
- ⁶M. Bockrath, D. H. Cobden, P. L. McEuen, N. G. Chopra, A. Zettl, A. Thess, and R. E. Smalley, *Science* **275**, 1922 (1997).
- ⁷P. G. Collins, A. Zettl, H. Bando, A. Thess, and R. E. Smalley, *Science* **278**, 100 (1997).
- ⁸Z. Yao, H. W. C. Postma, L. Balents, and C. Dekker, *Nature (London)* **402**, 273 (1999).
- ⁹M. S. Fuhrer, J. Nygård, L. Shih, M. Forero, Y.-G. Yoon, M. S. C. Mazzoni, H. J. Choi, J. Ihm, S. G. Louie, A. Zettl, and P. L. McEuen, *Science* **288**, 494 (2000).
- ¹⁰V. Derycke, R. Martel, J. Appenzeller, and P. Avouris, *Nano Letters* **1**, 453 (2001).
- ¹¹A. Bachtold, P. Hadley, T. Nakanishi, and C. Dekker, *Science* **294**, 1317 (2001).
- ¹²The iron nanoparticle catalyst was prepared following Ref. 13. The catalyst was reduced at 900°C in flowing H_2/Ar , followed by growth under pure methane flowing at 3500 sccm for 6 min. An alumina substrate coated with iron/molybdenum catalyst prepared as in Ref. 14 placed upstream from the substrate was found to promote NT growth.
- ¹³J. H. Hafner, C. Chin-Li, T. H. Oosterkamp, and C. M. Lieber, *J. Phys. Chem. B* **105**, 743 (2001).
- ¹⁴J. Kong, H. T. Soh, A. Cassell, C. F. Quate, and H. Dai, *Nature (London)* **395**, 878 (1998).
- ¹⁵I. A. Glavatskikh, V. S. Kortov, and H.-J. Fitting, *J. Appl. Phys.* **89**, 440 (2001).
- ¹⁶J. P. Vigouroux, J. P. Duraud, A. Le Moei, C. LeGressus, and D. L. Griscom, *J. Appl. Phys.* **57**, 5139 (1985).
- ¹⁷O. C. Wells, *Scanning Electron Microscopy* (McGraw-Hill, New York, 1974).